Thermodynamics of dimerization in solution as a rational tool for inducing nematic *vs.* smectic organizations in lanthanidomesogens†

Thomas B. Jensen,[a] Emmanuel Terazzi,[b] Bertrand Donnio,[b] Daniel Guillon[b] and Claude Piguet*[a]

Received (in Cambridge, UK) 26th September 2007, Accepted 30th October 2007
First published as an Advance Article on the web 6th November 2007
DOI: 10.1039/b714861e

The judicious tuning of simple thermodynamic parameters controlling dimerization processes in solution induces a rational switch between smectic and nematic organizations in thermotropic lanthanide-containing liquid crystals.

The design of modern functional (supra)molecular devices requires the combination of several components within nanometric objects, whose large sizes and limited anisometries limit their successful incorporation into responsive (*i.e.* switchable) macroscopic environments such as thermotropic liquid crystals.[1] However, the empirical observation that the connection of diverging flexible polycatenar[2] or dendrimeric[3] units to the central nanometric core produces low-temperature melting processes, allowed the recent incorporation of a series of uncommon supramolecular entities, such as electrochemically active fullerene,[4] mechanically mobile [2]catenane[5] and optically addressable lanthanide complexes,[6] into thermotropic cubic, columnar and lamellar mesophases. The origin of this behaviour can be rationalized with a simple thermodynamic model considering the successive melting (solid or glass → liquid crystal phase transition occurring at the temperature T_m) and clearing processes (liquid crystal → isotropic fluid phase transition occurring at the temperature T_c), as the result of the stepwise decorrelations of the flexible chains ($T_m = \Delta H_m/\Delta S_m$) and of the rigid cores ($T_c = \Delta H_c/\Delta S_c$), respectively.[6b,c] Consequently, the low melting temperatures T_m evidenced for polycatenar and dendrimeric units can be assigned to the large entropic gain accompanying the decorrelation of the divergent flexible chains.[7] This concept is well illustrated by the connection of the dendrimeric synthon R^0 to bulky fullerene[8] or of synthon R^1 to lanthanide complexes (Ln is a trivalent 4f-block ion),[9] which induces the formation of stable thermotropic smectic A mesophases (Scheme 1). The layered organization in the mesophase of these dendrimers has been attributed to attractive enthalpic intermolecular interactions operating between the terminal cyanobiphenyl groups, which are optimized for smectic arrangements. Moreover, the consequent parallel location of adjacent polarizable fullerenes or of polyaromatic aromatic lanthanide rigid cores in the smectic organization of these dendrimers may further contribute to improve the intermolecular attractive forces by dispersive interactions. Building on this reasoning, we infer that the fluidic nematic organization, which is rarely found in lanthanidomesogens (*i.e.* lanthanide-containing liquid crystals)[6] despite its suitability for practical applications, may be rationally induced in these dendrimeric mesogens assuming that enthalpic intermolecular interactions are reduced in order to allow an easier slipping of the (supra)molecules with respect to each others.

A preliminary support for this assumption can be found in the drastic disymmetrization of the rigid core produced by the connection of a single dendrimeric unit on one side of a bulky lanthanide dendritic complex, which promotes nematic organization in the mesophase.[6a] However, a tunable design requires a rational evolution from smectic A (SmA) toward nematic (N) *via* the stepwise loss of enthalpic intermolecular cohesions produced by the connection of an increasing number of sterically demanding methyl groups on the periphery of the terminal cyanobiphenyls in the synthon R^2 (Scheme 1). This challenge can be addressed with the synthesis of the ligand $\mathbf{Me_4L}$, which differs from the original ligand **L** in the attachment of four peripheral methyl groups at the *ortho*-positions of the terminal cyano biphenyl units (Scheme 2).[9]

The synthon **2b** was synthesized in 66% overall yield in six steps from the methylated precursor **1b**[10] using the same strategy previously reported for **2a**.[8,9] Coupling of either **2a** or **2b** with the tridentate coordination unit **3**[11] using EDCI/DMAP gave ligands **L**[9] and $\mathbf{Me_4L}$ in good yield (Scheme 2). Finally, reaction of $\mathbf{Me_4L}$ with $Ln(NO_3)_3$ gives complexes of overall stoichiometry $[Ln(\mathbf{Me_4L})(NO_3)_3]$, strictly similar to those previously characterized for $[Ln(\mathbf{L})(NO_3)_3]$.[9]

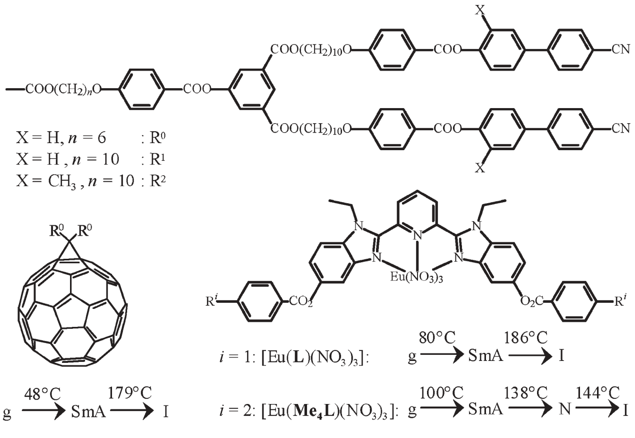

Scheme 1 Structure of dendrimeric mesogens and thermal behaviours (g = glass, SmA = smectic A, N = nematic, I = isotropic liquid).

---

[a] *Department of Inorganic, Analytical and Applied Chemistry, University of Geneva, 30 quai E. Ansermet, CH-1211, Geneva 4, Switzerland. E-mail: Claude.Piguet@chiam.unige.ch; Fax: (+41) 22 379 6830*
[b] *Groupe des Matériaux Organiques, Institut de Physique et Chimie des Matériaux de Strasbourg-IPCMS, 23 rue du Loess, B.P. 43, F67034, Strasbourg Cedex 2, France*

† Electronic supplementary information (ESI) available: Synthesis of $\mathbf{Me_4L}$, SAXS results, NMR spectra of $\mathbf{Me_4L}$ and of its complexes, van't Hoff plots, figures of ligand distribution for equilibrium (1), DSC and POM results. See DOI: 10.1039/b714861e

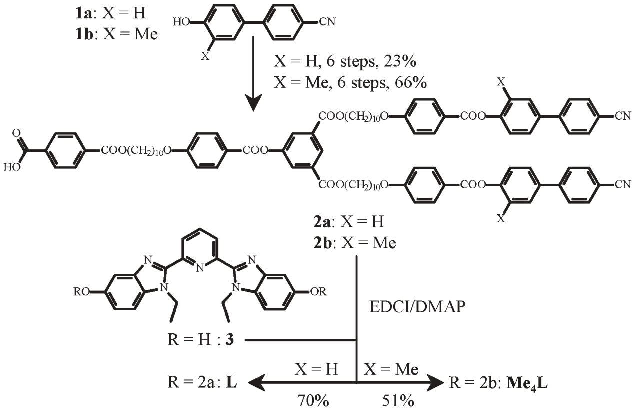

Scheme 2 Synthesis of the ligand $\mathbf{Me_4L}$.

In order to quantitatively explore the effect of the methylation process on the enthalpic intermolecular interactions in going from $[Ln(\mathbf{L})(NO_3)_3]$ to $[Ln(\mathbf{Me_4L})(NO_3)_3]$, the dimerization process shown in equilibrium 1 has been investigated by variable-temperature ^{1}H NMR in non-coordinating CD_2Cl_2 (total ligand concentration: C_{tot} = 0.01 M).

$$2\,[Ln(\mathbf{Me_4L})(NO_3)_3] \leftrightarrows [Ln_2(\mathbf{Me_4L})_2(NO_3)_6];\ K_{dim} \qquad (1)$$

As previously established for $[Eu(\mathbf{L})(NO_3)_3]$,[9] the ^{1}H NMR spectrum of $[Eu(\mathbf{Me_4L})(NO_3)_3]$ displays two sets of signals with different intensities (Fig. S1, see ESI†) corresponding to the monomeric and dimeric complexes of equilibrium (1). Integration of the signals of the two species at different temperatures gives their concentrations, from which the equilibrium constants K_{dim} and the thermodynamic parameters ΔH_{dim} and ΔS_{dim} can be calculated (Table 1, van't Hoff plots are shown in Fig. S2 in ESI†).

As expected, the connection of the methyl groups in $[Eu(\mathbf{Me_4L})(NO_3)_3]$ significantly reduces the intermolecular interactions between the cyanobiphenyl groups as measured by the significant decrease of the absolute value of $|\Delta H_{dim}|$ observed in going from $[Eu(\mathbf{L})(NO_3)_3]$ to $[Eu(\mathbf{Me_4L})(NO_3)_3]$. The associated increase in motion in the dimer is obviously associated with a concomitant increased disorder, which is evidenced by the less unfavorable entropy of dimerization found for $[Eu(\mathbf{Me_4L})(NO_3)_3]$, a typical case of enthalpy/entropy compensation (Table 1).[7] Consequently, the critical temperature $T_{50\%}$ at which the monomers $[Eu(\mathbf{L})(NO_3)_3]$ or $[Eu(\mathbf{Me_4L})(NO_3)_3]$ correspond to 50% of the ligand distribution in solution are similar (Table 1), but the temperature-induced dimer to monomer transformation is quite different for the two complexes and it displays a more abrupt slope for $[Eu(\mathbf{L})(NO_3)_3]$ (see Fig. S3 in ESI†). Interestingly, the intermolecular enthalpic cohesion in the dimer $[Eu_2(\mathbf{Me_4L})_2(NO_3)_6]$ does not exclusively rely on the terminal cyanobiphenyl groups, and the large increase of $|\Delta H_{dim}|$ observed in going from $[Eu(\mathbf{Me_4L})(NO_3)_3]$ to $[Pr(\mathbf{Me_4L})(NO_3)_3]$ is diagnostic for the formation of additional stabilizing nitrate bridges between large Ln(III), a phenomenon previously well-established for $[Ln(\mathbf{L})(NO_3)_3]$ (Ln = La–Eu).[11] Following this reasoning, the small nine-coordinate Lu(III) in $[Lu(\mathbf{Me_4L})(NO_3)_3]$ would display a much weaker enthalpic cohesion, strictly limited to intermolecular interactions between the methyl-substituted terminal cyanobiphenyls. We were thus not surprised that the dimerisation processes (eqn (1)) is not detected for the Lu-complex in CD_2Cl_2, which exists in its monomeric form in solution.

Table 1 Thermodynamic parameters for equilibrium (1) in CD_2Cl_2

Compound^a	ΔH_{dim}/ kJ mol^{-1}	ΔS_{dim}/ J mol^{-1} K^{-1}	K_{dim} (298 K)	$T_{50\%}{}^b$/ °C
$[Eu(\mathbf{L})(NO_3)_3]$	−55(4)	−166(11)	9	−4
$[Eu(\mathbf{Me_4L})(NO_3)_3]$	−25(1)	−58(5)	23	−13
$[Pr(\mathbf{Me_4L})(NO_3)_3]$	−33(4)	−72(14)	121	26

^{a} Data for complexes with **L** are taken from ref. 9. ^{b} $T_{50\%} = \Delta H_{dim}/(\Delta S_{dim} + R\ln C_{tot})$ is the critical temperature at which the monomer represents 50% of the ligand distribution in CD_2Cl_2 (C_{tot} = 0.01 M).

Having established that both the reduced size of Ln(III) and the methylation of the ligand backbone decrease the enthalpy of dimerization for the complexes in a non-coordinating solvent, we can infer that the formation of thermotropic nematic mesophases will be favored for the methylated complexes $[Ln(\mathbf{Me_4L})(NO_3)_3]$ with small metals, because closely related intermolecular interactions operate in the bulk materials. The thermal behaviour of the ligand $\mathbf{Me_4L}$ and of its complexes have been thus investigated by using a combination of differential scanning calorimetry (DSC), polarized optical microscopy (POM) and small-angle X-ray scattering (SAXS). The results are summarized in Table 2 (for details see Tables S1, S2 and Fig. S4, S5 in ESI†).

In agreement with our predictions, the connection of methyl groups in going from **L** to $\mathbf{Me_4L}$ leads to a 12% decrease of the clearing enthalpy ΔH_c (and a concomitant 41 °C shift of the clearing temperature), which results from the weakened intermolecular interactions involving cyanobiphenyl units in $\mathbf{Me_4L}$. Lower clearing temperatures are also systematically observed for the complexes $[Eu(\mathbf{Me_4L})(NO_3)_3]$ and $[Lu(\mathbf{Me_4L})(NO_3)_3]$ upon comparison with their non-methylated analogues, but the most striking consequence of the reduced intermolecular cohesion concerns the eventual programmed formation of enantiotropic fluidic nematic mesophases for the methylated complexes (Table 2 and Fig. 1, and Fig. S4 in ESI†).

Table 2 Phase transition temperatures and associated enthalpy and entropy changes for **L**, $\mathbf{Me_4L}$ and their complexes

Compound^a	Transition^b	T/°C	ΔH/ kJ mol^{-1}	ΔS/ J mol^{-1} K^{-1}
L	g → N	52		
	N → I	238	11.0	21.5
$\mathbf{Me_4L}$	g → N	50–70^c		
	N → I	197	9.7	20.5
$[Eu(\mathbf{L})(NO_3)_3]$	g → SmA	80		
	SmA → I	186	11.1	24.2
$[Eu(\mathbf{Me_4L})(NO_3)_3]$	g → SmA	90–110^c		
	SmA → N	138	2.4	5.8
	N → I	144	4.9	11.8
$[Lu(\mathbf{L})(NO_3)_3]$	g → SmA	100		
	SmA → PCr	150		
	PCr → SmA	170		
	SmA → I	200	3.3	6.9
$[Lu(\mathbf{Me_4L})(NO_3)_3]$	g → SmA	90–110^c		
	SmA → N	130	0.8	1.9
	N → I	144	6.9	16.4

^{a} Data for **L** and for its complexes are taken from ref. 9. ^{b} g = glass; SmA = smectic A phase; N = nematic phase; I = isotropic fluid; PCr = partially crystallized. ^{c} Transition temperature measured by POM.

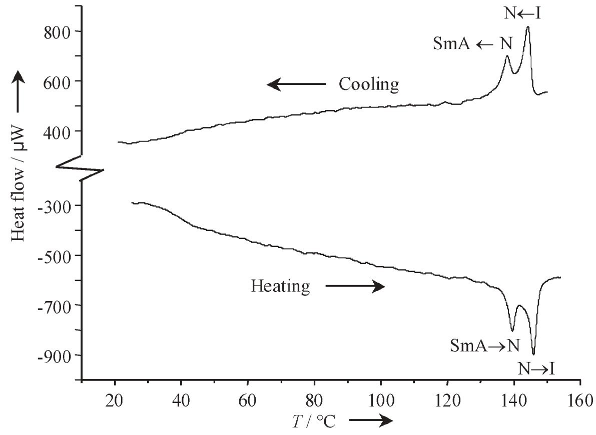

Fig. 1 DSC trace of [Eu(**Me$_4$L**)(NO$_3$)$_3$] (5 °C min^{-1} under N$_2$).

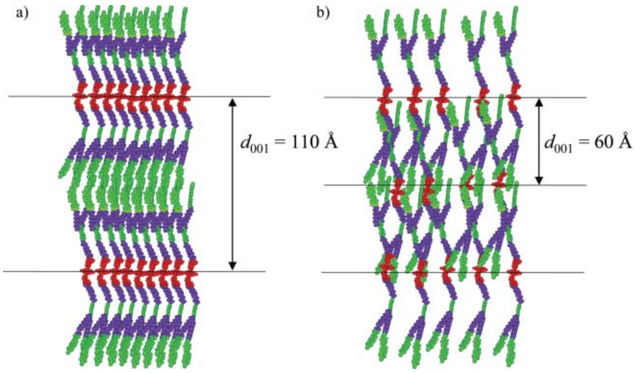

Fig. 2 Proposed organization in the SmA phases obtained by SAXS for (a) [Eu(**Me$_4$L**)(NO$_3$)$_3$] and (b) [Lu(**Me$_4$L**)(NO$_3$)$_3$]. Red: coordinating benzimidazole–pyridine–benzimidazole unit; green: other aromatic groups; violet: aliphatic chains.

In order to rationalize the thermodynamics of the SmA → N phase transition, we must first consider the organization of the molecules in the layered smectic A phase (SmA). For [Eu(**Me$_4$L**)(NO$_3$)$_3$] at 120 °C, the SAXS profile shows the *hkl* = 001 reflection (= interlayer distance) occurring at 110 Å, a length corresponding to the fully stretched complex molecule (Fig. 2(a)).[9] In sharp contrast, the *hkl* = 001 reflection for [Lu(**Me$_4$L**)(NO$_3$)$_3$] recorded at the same temperature indicates an interlayer separation of only 60 Å, which implies the alternative intertwined organization (Fig. 2(b)). This behaviour agrees with the trend of the larger central lanthanides (Ln = Eu) to form additional stabilizing nitrate bridges with adjacent neighbours (Fig. 2(a)), while the smaller lanthanides (Ln = Lu) cannot participate to this mode of intermolecular interactions (Fig. 2(b)).

The SmA → N phase transition is characterized by the collapse of the *hkl* = 001 and 002 reflections (Fig. S5, see ESI†), while a birefringent texture is maintained (Fig. S6, see ESI†). The stronger intermolecular cohesion observed in the SmA phase of [Eu(**Me$_4$L**)(NO$_3$)$_3$] requires ΔH = 2.4 kJ mol^{-1} to enter the nematic phase, while [Lu(**Me$_4$L**)(NO$_3$)$_3$], which displays less possibilities for intermolecular interactions in its SmA phase, requires only ΔH = 0.8 kJ mol^{-1}.

In conclusion we have succeeded in demonstrating that the simple thermodynamics of dimerization of molecules in non-coordinating solvents can be used as an efficient tool for programming and rationalizing the formation of smectic and nematic mesophases in lanthanidomesogens

We thank K.-L. Buchwalder for recording DSC and Drs L. Guénée and B. Heinrich for assistance with SAXS analysis. Financial support from the Swiss National Science Foundation is gratefully acknowledged.

Notes and references

1 (*a*) V. Balzani, A. Credi, F. M. Raymo and J. F. Stoddart, *Angew. Chem., Int. Ed.*, 2000, **39**, 3348–3391, (*Angew. Chem.*, 2000, **112**, 3484–3530); (*b*) V. Balzani, A. Credi and M. Venturi, *Chem.–Eur. J.*, 2002, **8**, 5525–5532; (*c*) A. Mulder, J. Huskens and D. N. Reinhoudt, *Org. Biomol. Chem.*, 2004, **2**, 3409–3424.
2 (*a*) B. Donnio and D. W. Bruce, *Struct. Bonding*, 1999, **95**, 194–247; (*b*) B. Donnio, B. Heinrich, H. Allouchi, J. Kain, S. Diele, D. Guillon and D. W. Bruce, *J. Am. Chem. Soc.*, 2004, **126**, 15258–15268.
3 (*a*) B. Donnio and D. Guillon, *Adv. Polym. Sci.*, 2006, **201**, 45–155; (*b*) B. Donnio, S. Buathong, I. Bury and D. Guillon, *Chem. Soc. Rev.*, 2007, **36**, 1495–1513.
4 R. Deschenaux, B. Donnio and D. Guillon, *New J. Chem.*, 2007, **31**, 1064–1073.
5 (*a*) E. Baranoff, J. Voignier, T. Yasuda, V. Heitz, J.-P. Sauvage and T. Kato, *Angew. Chem., Int. Ed.*, 2007, **46**, 4680–4683, (*Angew. Chem.*, 2007, **119**, 4764–4767); (*b*) I. Aprahamian, T. Yasuda, T. Ikeda, S. Saha, W. R. Dichtel, K. Isoda, T. Kato and J. F. Stoddart, *Angew. Chem., Int. Ed.*, 2007, **46**, 4675–4679, (*Angew. Chem.*, 2007, **119**, 4759–4763).
6 (*a*) T. Cardinaels, K. Driesen, T. N. Parac-Vogt, B. Heinrich, C. Bourgogne, D. Guillon, B. Donnio and K. Binnemans, *Chem. Mater.*, 2005, **17**, 6589–6598; (*b*) C. Piguet, J.-C. G. Bünzli, B. Donnio and D. Guillon, *Chem. Commun.*, 2006, 3755–3768; (*c*) K. Binnemans and C. Görller-Walrand, *Chem. Rev.*, 2002, **102**, 2303–2346.
7 A. Escande, L. Guénée, H. Nozary, G. Bernardinelli, F. Gumy, A. Aebischer, J.-C. G. Bünzli, B. Donnio, D. Guillon and C. Piguet, *Chem.–Eur. J.*, 2007, **13**, 8696–8713.
8 B. Dardel, D. Guillon, B. Heinrich and R. Deschenaux, *J. Mater. Chem.*, 2001, **11**, 2814–2831.
9 E. Terazzi, B. Bocquet, S. Campidelli, B. Donnio, D. Guillon, R. Deschenaux and C. Piguet, *Chem. Commun.*, 2006, 2922–2924.
10 Y. L. Bennani, R. Faghih, W. J. Dwight, A. Vasudevan and S. E. Conner, *US. Pat. Appl. Publ.* 2002, Ser. No. 902,925, CODEN: USXXCO US 2002137931 A1 20020926.
11 E. Terazzi, S. Torelli, G. Bernardinelli, J.-P. Rivera, J.-M. Bénech, C. Bourgogne, B. Donnio, D. Guillon, D. Imbert, J.-C. G. Bünzli, A. Pinto, D. Jeannerat and C. Piguet, *J. Am. Chem. Soc.*, 2005, **127**, 888–903.